Apoptosis (2019) 24:612–622
https://doi.org/10.1007/s10495-019-01544-w

Cellular responses of *BRCA1*-defective HCC1937 breast cancer cells induced by the antimetastasis ruthenium(II) arene compound RAPTA-T

Tidarat Nhukeaw[1] · Khwanjira Hongthong[1] · Paul J. Dyson[2] · Adisorn Ratanaphan[1]

Published online: 23 April 2019

Abstract
An organometallic ruthenium(II) arene compound, Ru(η^6-toluene)(PTA)Cl_2 (PTA = 1,3,5-triaza-7-phosphaadamantane), termed RAPTA-T, exerts promising antimetastatic properties. In this study, the effects of RAPTA-T on *BRCA1*-defective HCC1937 breast cancer cells have been investigated, and compared to its effects on *BRCA1*-competent MCF-7 breast cancer cells. RAPTA-T showed a very low cytotoxicity against both tested cells. Ruthenium is found mostly in the cytoplasmic compartment of both cells. Flow cytometric analysis reveals that the compound arrests the growth of both cells by triggering the G2/M phase that led to the induction of apoptosis. At equimolar concentrations, RAPTA-T causes much more cellular *BRCA1* damage in HCC1937 than in MCF-7 cells, suppressing the expression of *BRCA1* mRNA in both cell lines with the subsequent down-regulation of the BRCA1 protein. Interestingly, RAPTA-T exhibits an approximately fivefold greater ability to suppress the expression of the BRCA1 protein in HCC1937 than in MCF-7 cells. These data provide insights into the molecular mechanisms by which RAPTA-T exerts its effects on *BRCA1*-associated breast cancer cells.

Keywords Ruthenium complexes · BRCA1 · Breast cancer · Cell cycle · Apoptosis · BRCA1 expression

Introduction

Breast cancer is one of the most frequent malignant diseases and the second highest cause of cancer death among women worldwide [1]. In clinical settings, different responses to systemic therapy result from the complexity and heterogeneity of breast cancer with distinct histopathological, genetic and epigenetic characteristics [2, 3]. Recently, several studies have highlighted the level of the BRCA1 expression as a potential biomarker to manage patients and predict the response to specific therapies [4]. It has been reported that DNA repair of BRCA1-deficient cancer cells is defective due to a single mutant *BRCA1* allele. The mutation increases sensitivity to DNA damage-based chemotherapeutics through modulation of chromosomal aberrations and apoptosis [5–7]. In addition, cancer cells carrying *BRCA1* mutations and hypermethylation of *BRCA1* promoters with low BRCA1 expression have been shown to be hypersensitive to platinum-based DNA damaging agents, such as cisplatin and carboplatin, and to poly(ADP-ribose) polymerase (PARP) inhibitors, leading to effective clinical responses to *BRCA1*-associated breast cancers [8–11]. The neoadjuvant settings of platinum-based chemotherapy have shown a high rate of pathologic complete response (pCR) and a better disease free survival (DFS) and overall survival (OS) in breast cancer patients defective in *BRCA1*-mediated DNA repair of double-strand breaks (DSB) [12, 13].

However, a clinical trial of metastatic breast cancer patients treated with platinum-based chemotherapy revealed severe side effects that persist over a prolonged period of time [14, 15]. Furthermore, some breast cancers acquire resistance, in particular, with the induction of secondary mutations in the *BRCA1* gene [16, 17]. Consequently, alternative transition metal-based compounds with increased efficacy that overcome the problems associated with platinum-based chemotherapy are required. Compounds based on ruthenium are regarded as potential drug candidates [18, 19], with some

✉ Adisorn Ratanaphan
adisorn.r@psu.ac.th

1 Laboratory of Pharmaceutical Biotechnology, Department of Pharmaceutical Chemistry, Faculty of Pharmaceutical Sciences, Prince of Songkla University, Hat-Yai, Songkhla 90112, Thailand

2 Institute of Chemical Sciences and Engineering, Swiss Federal Institute of Technology Lausanne (EPFL), 1015 Lausanne, Switzerland

ruthenium(III) compounds already entering clinical trials [20]. Ruthenium(II) arene complexes combined with the 1,3,5-triaza-7-phosphaadamantane (PTA) ligand, termed RAPTA complexes, show promise as alternatives to platinum-based drugs. In general, RAPTA complexes are not strongly cytotoxic [21, 22], although the prototype compound, [Ru(η^6-*p*-cymene)(PTA)Cl_2], termed RAPTA-C (Fig. 1a), was shown to inhibit the growth of tumor cells extracted from mice bearing the Erlich ascites carcinoma (EAC) [23]. In vivo RAPTA-C has also been shown to exhibit a strong anti-tumor effect [21, 24–26]. Compared to platinum-based drugs the mode of action of RAPTA-C appears to be markedly different, with binding to histone proteins in nucleosome core particles rather than DNA [27, 28]. Ru(η^6-toluene)(PTA)Cl_2, termed RAPTA-T (Fig. 1b), is closely related to RAPTA-C, however, some evidence points toward adducts formed by RAPTA-T with guanine residues in double-stranded oligonucleotides [29]. RAPTA-T inhibits some steps of the metastatic process, including detachment from the primary tumor cell, migration, and re-adhesion with this effects apparently being mediated through interactions with components in the extracellular matrix [30]. It is also notable that the effects of RAPTA-T were more pronounced with the highly invasive MDA-MB-231 breast cancer cells compared to non-invasive MCF-7 cells or non-tumorigenic HBL-100 derived from breast tissue [31].

Recently, it has been shown that RAPTA-T causes upregulation of many cellular target proteins suggesting a broad mechanism of action involving suppression of both metastasis and tumorigenecity [32]. Furthermore, RAPTA-T displays strong in vivo antiangiogenic activity in the chicken chorioallantoic membrane model exemplified by a decrease in microvessel density [30]. RAPTA-T clearly has potential in the treatment of breast cancers, however, the activity of RAPTA-T against the *BRCA1*-defective HCC1937 breast cancer cells is unknown. Therefore, we have evaluated the effects of RAPTA-T on the *BRCA1*-defective HCC1937 breast cancer cells in comparison to *BRCA1*-competent MCF-7 breast cancer cells.

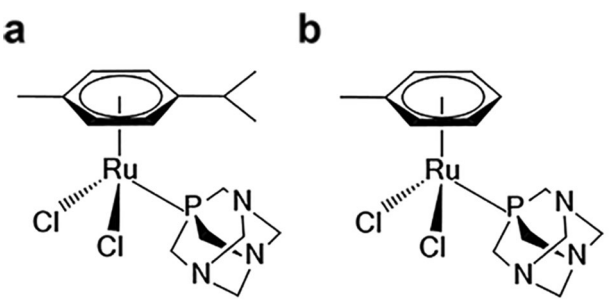

Fig. 1 Structures of RAPTA-C (**a**), RAPTA-T (**b**)

Materials and methods

Cell culture

HCC1937 (BRCA1 mutant, TNBC) and MCF-7 (wild-type BRCA1) breast cancer cell lines were obtained from the American Type Culture Collection (ATCC), Rockville, MD, USA. HCC1937 cells were cultured in RPMI 1640 medium (Life Technologies, Paisley, UK), while MCF-7 cells were cultured in Dulbecco's modified Eagle's medium (DMEM) (Life Technologies, Pawasley, UK). Both media were without phenol red and supplemented with 10% fetal bovine serum (FBS) and 1% penicillin-streptomycin. Both cell lines were incubated in a constant temperature of 37 °C incubator with a humidified atmosphere of 5% CO_2.

Antiproliferative effects

The cytotoxicity effect of RAPTA-T on HCC1937 and MCF-7 cells were performed using a colorimetric test based on the reduction of 3-(4,5-dimethylthiazol-2-yl)-2,5-diphenyl tetrazolium bromide (MTT) as previously described [33]. Briefly, the cell lines were plated at a density of 1×10^4 cells in 100 µl of cell culture media into each well of the 96 well microplates, and then cultured in 37 °C incubator for overnight. RAPTA-T complex was diluted with the required amount of cell culture media in order to desire various final concentration (0–1200 µM) and 200 µl of each concentration was added to respective wells in triplicate, following by incubation at 37 °C for 48 h. At the end of incubations, the treatments were removed and the cell lines were washed twice with 100 µl of phosphate-buffered saline (PBS) (pH 7.4). Then, 100 µl of 0.5 mg/ml MTT solution were added to each well and the plates were incubated for additional 4 h at 37 °C in dark conditions. Following the incubation the MTT solution was carefully removed. The insoluble formazan produced was by dissolved in 200 µl of DMSO and the absorbance of each well was measured at a wavelength of 570 nm using a microplate reader spectrophotometer. The percentage of cell viability was calculated with the absorbance values of the treated cells divided by the absorbance of untreated cells. The values of the half inhibitory concentration (IC_{50}) that reduced the number of living cells to 50% were determined by the correlation between the percentage of viability cells and the concentration curves.

Cellular accumulation and distribution

Cells were seed in 75 cm^3 cell culture flask at a density of 5×10^5 cells/ml and grown at 37 °C with 5% CO_2. The cells were treated with 1 mM of RAPTA-T [22] and then

incubated for 48 h. The cells were washed twice with PBS, harvested by trypsinization and centrifuged at 1000×*g* for 10 min at 4 °C. For cell fractionation, all operations were carried out in the cold (4 °C) [34]. The cultured cells were broken in a sucrose-mannitol medium. The homogenate was centrifuged at 1000×*g* for 10 min to yield a crude nuclear pellet and a crude cytoplasmic fraction. The nuclear pellet was resuspended in 250 mM sucrose in a Tris–Mg–NaCl buffer. The homogenate was mixed with 2 volumes of 2.3 M sucrose, and then centrifuged at 40,000×*g* for 30 min. The sediment nuclei were suspended in 250 mM sucrose in Tris–Mg–NaCl buffer containing 0.1% Triton X-100 (w/w) and centrifuged at 1000×*g* for 10 min. The pellet was suspended in 1% of a solution of sodium dodecyl sulfate (SDS) in 10 mM Tris–Cl (pH 8.0), 150 mM NaCl, 1 mM EDTA and kept overnight at room temperature. The solution was centrifuged at 17,000×*g* for 30 min and dissolved in double distilled water to yield the nuclear fraction. The cytoplasmic fraction was centrifuged at 12,000×*g* for 10 min to pellet the mitochondrial fraction and the cytoplasmic fraction. The mitochondrial pellet was rehomogenized in sucrose-mannitol medium. The suspension was centrifuged at 1000×*g* for 5 min, the precipitate was discarded and the mitochondria resedimented at 12,000×*g* for 10 min. The ruthenium contents in three fractions (cytoplasmic, mitochondrial and nuclear fraction) were analyzed by an inductively coupled plasma mass spectrometer (ICP-MS).

Cell cycle profiling analysis

About 10^6 cells were seeded into 6-well plates and further grown at 37 °C with 5% CO_2 until approximately 80% confluent. The medium was removed and cells were then exposed to completed medium containing 1 mM of RAPTA-T for 48 h. After the exposure period the cells were harvested by trypsinization, washed twice with cold PBS and centrifuged at 300×*g* for 5 min at 4 °C. The pellet was fixed with 70% ethanol in PBS overnight at − 20 °C. The fixed cells were washed with cold PBS. Following centrifugation the pellet was resuspended in 0.5 ml of PBS and stained with 1 ml of PBS containing 100 µg/ml of RNase A, 50 µg/ml of PI, and 0.1% of Triton-X 100), and then further incubated at 37 °C in the dark for 30 min. The DNA content was quantitated by counting 20,000 cells and expressed as G0/G1, S, and G2/M phases.

Annexin V apoptosis detection

After 10^6 cells were exposed to 1 mM of RAPTA-T for 48 h. Cells were trypsinised, washed twice with cold PBS, and centrifuged. The supernatant was discarded and 100 µl of 1 × Annexin-binding buffer was added to resuspend the pellets. Then, 5 µl of Alexa Fluor 488 annexin V and 1 µl of PI (100 µg/ml) was added to each cell suspension and mixed gently, and further incubated at room temperature in the dark for 15 min. Subsequently, 400 µl of 1 × Annexin-binding buffer was added and mixed gently. Annexin V binding was analyzed by the FACS flow cytometer with a fluorescence emission at 530 and 575 nm using fluorescence excitation at 488 nm. The percentage of apoptotic cells was calculated from the total 20,000 cells.

Semi-quantification of cellular *BRCA1* damage using QPCR method

After 10^6 cells were incubated with the various concentration of RAPTA-T (200–1200 µM) the genomic DNA of the ruthenium-treated and untreated cells (control) was isolated, and the 3426 bp fragment of the *BRCA1* exon 11 of the cells was then amplified in a PCR reaction [35, 36]. Briefly, PCR reactions were carried out in a total volume of 50 µl containing 400 ng of a treated genomic DNA template, 0.5 µM of forward primer (5′-GCCAGTTGGTTGATTTCCACC -3′) and reverse primer (5′-GTAAAATGTGCTCCCC AAAAG -3′), 300 µM of each dNTP, 2 units of Phusion Hot Start DNA polymerase, 1.5 mM $MgCl_2$, 1xPhusion™ GC Buffer and steriled water to make up to 50 µl. The 3426 bp fragment of the *BRCA1* exon 11 of the cells was then amplified using thermal cycle conditions as the following: 3 min at 94 °C; 30 cycles of 30 s at 94 °C, 2 min at 72 °C, and a final extension for 7 min at 72 °C. The PCR products were separated on 1% agarose gel electrophoresis, stained with ethidium bromide and visualized under UV light. The quantitative PCR (QPCR) method was used to assess the DNA polymerase blocking effect of the ruthenated DNA adduct. The amplification products were quantified using a Bio-Rad imaging densitometer, and the amount of DNA amplification (%) was plotted as the concentrations of

RAPTA-T. The number of lesions per the 3426 bp fragment of the *BRCA1* exon 11 was estimated by the Poisson equation [36],

$$S = -\ln\left(A_d/A\right)$$

where S is the lesion frequency per strand, A is the absorbance unit produced from a given amount of non-damaged DNA template, and A_d is the absorbance unit from a given amount of damaged DNA template (damaged by a particular concentration of RAPTA-T). Therefore, A_d/A is the radio of non-damaged DNA template at a given concentration.

Quantification of *BRCA1* mRNA expression using real-time quantitative RT-PCR

After 10^6 cells were incubated in the absence and the presence of 1 mM of RAPTA-T for 48 h 37 °C with 5% CO_2 the cells were harvested, and then the total RNA was isolated

from the culture cells using the RNeasy® Mini Kit (Qiagen, Germany). One microgram of total RNA was reverse-transcribed for cDNA strand complementary by using QuantiTech® Reverse Transcription (Qiagen, Germany). The primer sequences for RT-PCR were used follows; *BRCA1*: 5′-GCCAGTTGGTTGATTTCCACC-3′ (forward) and 5′GTCAAATGTGCTCCCCAAAAGC-3′(reverse); *β-Actin:* 5′-CCGTAAAGACCTCTATGCCAACA-3′ (forward) and 5′-CGGACTCATCGTACTCCTGCT-3′ (reverse). Real-time PCR reactions were then carried out in a total volume of 25 µl including 100 ng of the cDNA template, 12.5 µl of QuantiFast SYBR green PCR master mix, and the final concentration of primers of 0.5 µM. The PCR conditions were as follows: 5 min at 95 °C, and 35 cycles of 10 s at 95 °C, 30 s at 60 °C. Fluorescence was measured during the annealing step on an ABI-Prism 7300 analytical thermal cycler (Applied Biosystems). Data were analyzed according to the 2-ΔΔCq method [37], and normalized by β-Actin mRNA expression in each sample.

Quantification of BRCA1 protein expression using Western blot

After 10^6 cells were incubated in the absence and the presence of 1 mM of RAPTA-T for 48 h 37 °C with 5% CO_2 the cells were washed twice with PBS, pelleted, and lysed with 200 µl of lysis buffer (50 mM Tris-HCI (pH 8.0), 5 mM NaCl, 2% SDS, 5 mM EDTA, 1% Triton®X-100, 100 mM PMSF) for 5 min and spun at 16,000×*g* for 10 min at 4 °C. The supernatant was transferred to determine the protein concentration by a Bradford assay. Whole-cell extracts were fractioned through a 6% SDS-polyacrylamide gel electrophoresis. The separated protein was then transferred to the nitrocellulose membrane in a transfer buffer (3.03 g of Tris base, 14.4 g of glycine, 200 ml of methanol, and double distilled water adjusted to 1 L) and layered on the semi-dry electroblotter for 6 h. The blot was blocked with a TBS buffer containing 10% bovine serum albumin (BSA) for 4 h with shaking and the membrane was then incubated with primary antibody, anti-BRCA1 (Ab-1) mouse (MS110) antibody at a dilution of 1:1000 in 10% BSA in TBS buffer for 4 h with shaking. An equivalent protein loading was controlled by β-actin expression using anti β-actin at a dilution of 1:1500 in 10% BSA in TBS buffer for 4 h with shaking. The blot was then washed by washing buffer, Tris buffered saline with Tween®20 (TBST) 8 times for 5 min, then exposed to an anti-mouse IgG horseradish conjugated secondary antibody at a dilution of 1:1000 in 10% BSA in TBS for 1 h with shaking. The blot was washed by TBST 8 times for 5 min, then visualized by enhanced chemiluminescence. The enhanced chemiluminescence working solution was prepared by mixing equal parts of two substrate components of the stable peroxide solution and the Lumino/Enhancer solution to the final volume of 0.1 ml/cm^2 of the blot. The blot was incubated with the working solution for 5 min, then dried and exposed to an X-ray film in a film cassette.

Data processing and statistical analysis

Statistical analysis of the results was performed using one-way ANOVA and Turkey's post-test for comparisons with a control. A probability of 0.01 deemed statistically significant. The following notation was used throughout the manuscript: $*p < 0.01$, relative to the control.

Results

Antiproliferative effect of RAPTA-T on human breast cancer cells, cellular uptake and distribution

The effect of RAPTA-T on cell growth inhibition of MCF-7 and HCC1937 cells was initially evaluated using the MTT assay. The percentage of cell viability after exposure to various concentration of RAPTA-T for 48 h was estimated, see Fig. 2. RAPTA-T exhibits a dose-dependent inhibitory effect of cell growth against MCF-7 and HCC1937 cells. No significant difference of cell viability was observed in both breast cancer cell lines at the same concentrations. To investigate intracellular ruthenium content and distribution in the cytoplasm, mitochondria and nuclear fraction in MCF-7 and HCC1937 cells, 1 mM of RAPTA-T was incubated with the cells for 48 h and then the three cellular compartments were separated and the ruthenium content of each fraction determined using ICP-MS. The ruthenium accumulates mostly in the cytoplasm, i.e. 70 and 90% in the MCF-7 and HCC1937 cells, respectively (Fig. 3). Furthermore, ruthenium was also detected in nuclear fraction and some in the mitochondrial fraction. There is more ruthenium present in the nuclear fraction of MCF-7 cells than in HCC1937 cells, i.e. 31% and 7%, respectively.

Cell cycle arrest and mechanism of cell death

The effect of RAPTA-T on the cell cycle distribution and cancer cell death was analyzed by flow cytometry. After treatment the cells with the 1 mM of RAPTA-T for 48 h, the DNA content was estimated by propidium iodide staining. RAPTA-T treatment results in an increase in the population of the cells in G2/M cell cycle phase of MCF-7 and HCC1937 cells, accounting for 17.3% and 29.4%, respectively, compared to the control (Fig. 4a, b). These results show that RAPTA-T progressively induces G2/M cell cycle arrest in both cell lines, along with the dramatically decreased cell population in the G0/G1 and S phase. Annexin V and PI double staining was used to determine

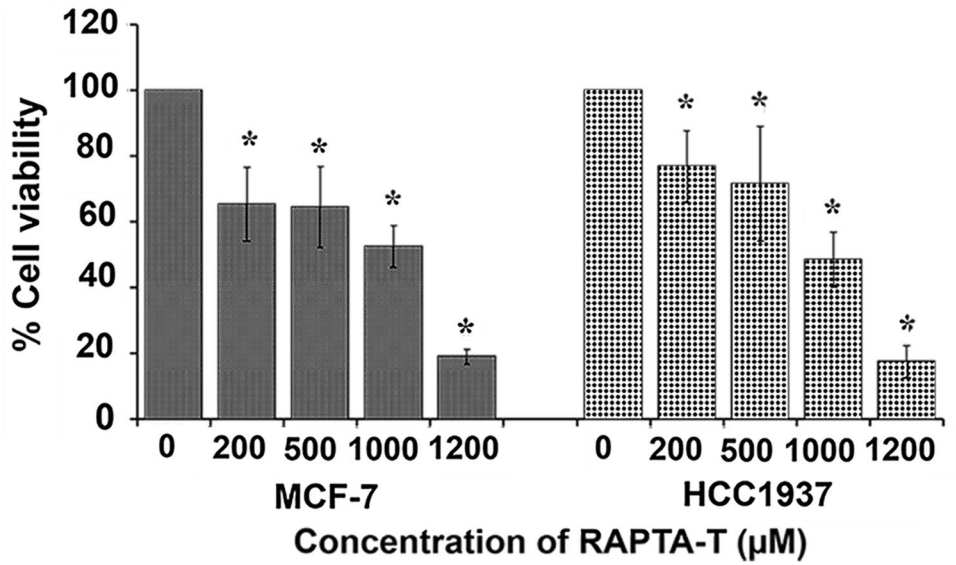

Fig. 2 The antiproliferative effect of RAPTA-T on MCF-7 and HCC1937 cells. Cells were treated with various concentration of RAPTA-T for 48 h and then the percentage of viable cells was assessed using the MTT assay. Experiments were performed in triplicate. Statistically significance differences from the untreated control are indicated by $*p < 0.01$

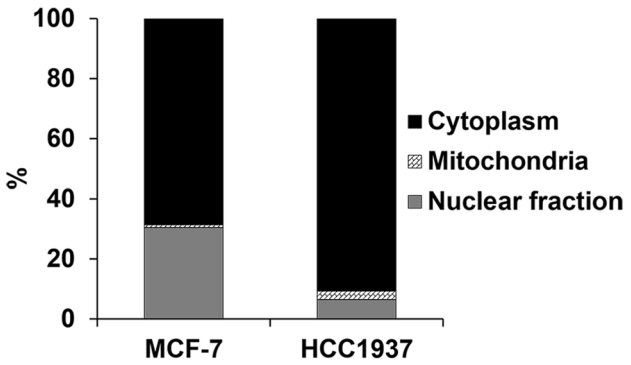

Fig. 3 Intracellular accumulation and distribution of RAPTA-T in MCF-7 and HCC1937 cells. Cells were exposed to 1 mM of RAPTA-T for 48 h. The cytoplasm, mitochondria, and nuclear fraction compartments were isolated and the ruthenium content of each compartment was quantified using ICP-MS and presented as the percentage distribution relative to the total ruthenium content detected

RAPTA-T induced apoptotic cell death. The percentage of total apoptotic cells calculated by the sum of both early and late apoptotic cells is shown in Fig. 5, indicates that RAPTA-T is able to induce apoptosis in both cell lines to a similar extent.

RAPTA-T reduces *BRCA1* replication in BRCA1-defectifve HCC1937 cells

A quantitative PCR-based (QPCR) assay was used to investigate the effect of RAPTA-T on cellular *BRCA1* damage in MCF-7 and HCC1937 cells after exposure to various concentration of RAPTA-T for 48 h. After treatment, genomic DNA of the ruthenium-treated or untreated (control) cells was extracted, and the 3426 bp fragment of *BRCA1* exon 11 of the cells was then amplified by PCR that utilized the ruthenated *BRCA1* adducts as templates to monitor the progress of DNA polymerization [33]. RAPTA-T exhibited a dose-dependent inhibition of *BRCA1* amplification in both breast cancer cell lines (Fig. 6a). The amount of *BRCA1* amplification was inversely proportional to the amount of Ru-DNA lesions within the specified DNA region. RAPTA-T showed different capacities to block replication of the *BRCA1* exon 11 of MCF-7 and HCC1937 cells. At equimolar concentrations RAPTA-T causes considerably more damage to the HCC1937 cells than the MCF-7 cells. The inhibition concentration for 50% *BRCA1* amplification by RAPTA-T was at 600 μM for HCC1937 cells and in MCF-7 cells above 1200 μM (Fig. 6b).

Lesion induction within the 3426 bp fragment of the *BRCA1* exon 11 can be quantitated by assuming a random (Poisson) distribution of damage. The amount of Ru-DNA lesions were calculated using a Poisson equation. The relationship between the ruthenium concentration and the ruthenium ions bound to the 3426 bp fragment of the *BRCA1* exon 11 in MCF-7 and HCC1937 cells is shown in Fig. 6c. The results reveal an approximately threefold higher rate of ruthenation in MCF-7 cells compared to HCC1937 cells under equivalent experimental conditions.

Downregulation of *BRCA1* mRNA expression and protein expression

Real time quantitative PCR method was used to determine whether *BRCA1* transcription is inhibited by RAPTA-T. The level of *BRCA1* mRNA expression, after incubation of MCF-7 and HCC1937 cells with 1 mM of RAPTA-T for 48 h, decreased only in HCC1937 cells, while no significant alteration of *BRCA1* mRNA expression was

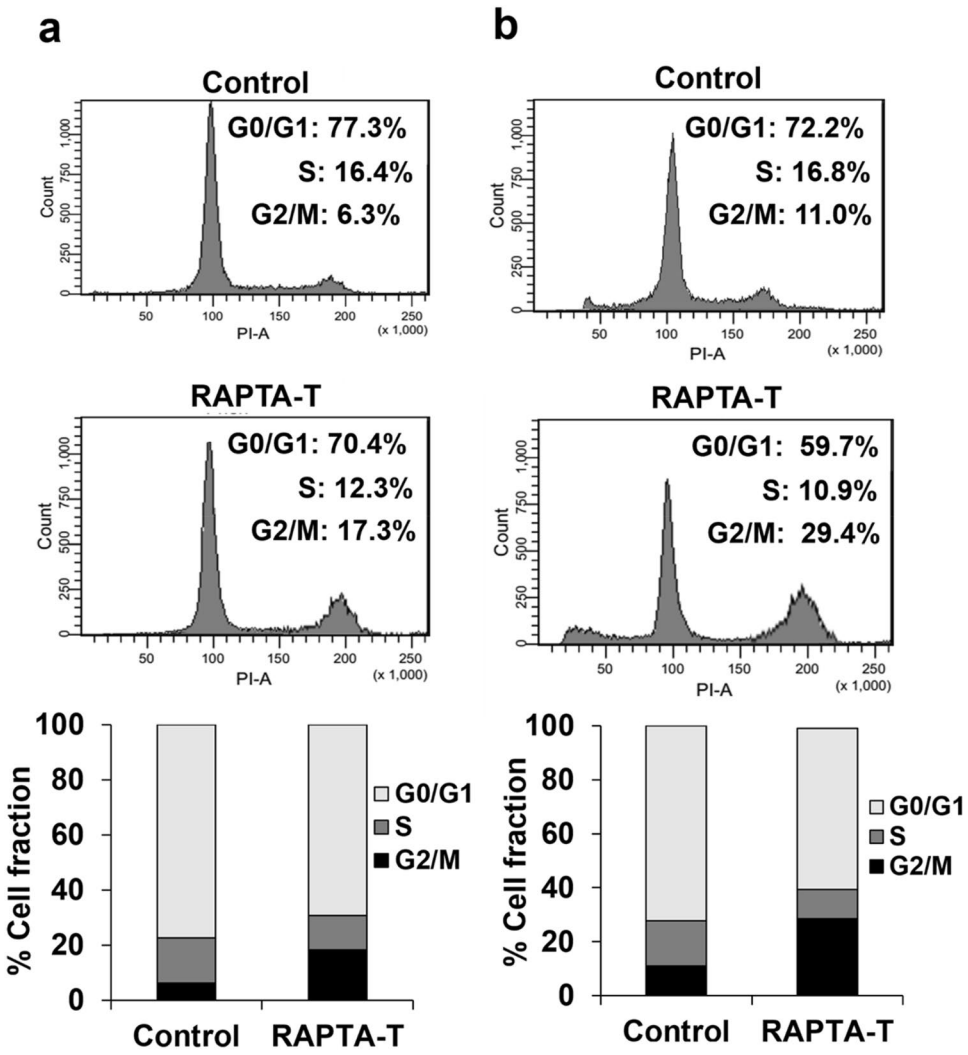

Fig. 4 Effect of RAPTA-T on the cell cycle distribution of MCF-7 (**a**) and HCC1937 (**b**) cells. Cells were incubated in the absence and the presence of 1 mM of RAPTA-T for 48 h and the DNA content was measured by PI staining. The percentage of 20,000 cells in the G0/G1, S, and G2/M phases were analyzed by fluorescence-activated cell sorting (FACS) analysis

observed in MCF-7 cells ($p < 0.01$) (Fig. 7a). However, reduced expression of *BRCA1* mRNA in HCC1937 cells represents an approximately twofold greater sensitivity to RAPTA-T compared to MCF-7 cells (Fig. 7b). Further investigations regarding the effect of RAPTA-T on the expression of the BRCA1 protein were performed using Western blot analysis, showing that RAPTA-T causes a similar reduction of the BRCA1 protein in both types of breast cancer cells (Fig. 8a). RAPTA-T exhibits an approximately fivefold greater ability to suppress the expression of the BRCA1 protein in the HCC1937 cells compared to the MCF-7 cells (Fig. 8b). These findings are consistent with previous investigations regarding the inhibition of *BRCA1* replication and transcription, in that the *BRCA1*-deficient HCC1937 cells are more sensitive to RAPTA-T than the *BRCA1*-competent MCF-7 cells.

Discussion

We investigated the effects of RAPTA-T on *BRCA1*-defective HCC1937 breast cancer cells in comparison to *BRCA1*-competent MCF-7 breast cancer cells. RAPTA-T displays a very low cytotoxicity in vitro against both selected breast cancer cell lines. Nevertheless, RAPTA-T was found to exhibit promising in vivo antimetastatic and antiangiogenic properties [22, 27]. Some evidence indicates that RAPTA compounds work on molecular targets other than DNA, implying a biochemical mode of action profoundly different to classical platinum anticancer drugs [27, 38–40]. Ruthenium was found to preferentially accumulate in the cytoplasm of MCF-7 and HCC1937 cells, which indicates that RAPTA-T might directly interacts

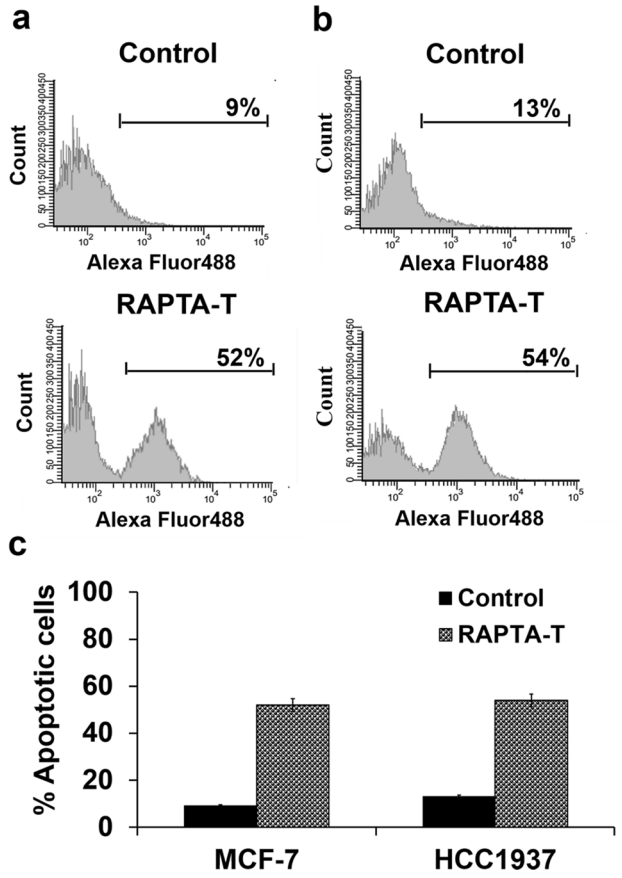

Fig. 5 Effect of RAPTA-T on apoptosis cell death of MCF-7 (**a**) and HCC1937 (**b**) cells. Cells were incubated in the absence and the presence of 1 mM of RAPTA-T for 48 h. The percentage of apoptotic cells was detected by analyzing for the Annexin V-FITC and PI binding using flow cytometry presented by the sum of the early apoptotic cells (Annexin V+/PI−) and late apoptotic cells (Annexin V+/PI+). The standard error of experiments realized in duplicate was plotted as shown in a bar graph (**c**)

with the transferrin membrane receptor and interfere with cellular specific proteins involved in the signal transduction pathways, cell adhesion, and migration processes that are likely to be critical to its mode of action [23, 41, 42]. Recent identification of key protein targets involved in the mechanism of action of RAPTA-T led to the identification of upregulation of a large number of cancer-related proteins that might be responsible for its ability to suppress metastasis and tumorigenicity. These data suggest that RAPTA-T could improve cancer drug chemotherapy combinations [32].

It is known that PARP-1 is an essential protein in DNA repair process associated with cancer resistance to chemotherapy and has been identified as potential drug target for cancer therapy [43]. The inhibition activity of PARP-1 by RAPTA-T was found to inhibit the activity of the PARP-1 enzyme to a similar extent of the benchmark inhibitor 3-aminobenzamide, suggesting that zinc-finger domains of PARP-1 might be altered by RAPTA-T that could be linked to its mode of action and potential molecular target in cancer treatment [44]. Similarly, a previous in vitro study has shown that RAPTA-T binds BRCA1 RING domain protein and result in change in conformation of the BRCA1 protein, leading to inactivation of the BRCA1-mediated ubiquitin ligase function. It is possible that cellular BRCA1 RING domain protein may also be a potential molecular target of RAPTA-T in cancer treatment [45]. These studies suggest that RAPTA-T is able to interact with a large number of key proteins. This broad action is important as it may lead to a widespread modification of cellular target proteins with effects on resistance and sensitizing that could be linked to antimetastatic and antitumor properties [38]. The modification of cellular targeted protein could be useful for cancer chemotherapy drug combination to improve their efficacy [32]. In addition, there is a higher content of ruthenium in the nuclear fractions of MCF-7 cells relative to HCC1937 cells where the RAPTA-T presumably forms adducts including genomic DNA and specific histone sites on the nucleosome core [29, 42]. Indeed, synergy between RAPTA-T and a gold-based drug, auranofin, was identified, with RAPTA-T allowing auranofin to form histone adducts by binding to distant histone sites, resulting in a synergistic activity in killing cancer cells [46].

During chemotherapy cellular or DNA damage responses mediated by various cell cycle checkpoints either activates specific DNA-repair machinery, resulting in the arrest of the cell cycle, or induces cellular apoptosis, when DNA damage seems irreparable. Flow cytometric analysis indicated that RAPTA-T influences cell cycle progression in both breast cancer cell lines, mainly by inducing arrest in the G2/M, which is accompanied by a corresponding reduction in the number of cells in the G0/G1 and S phases. RAPTA-T was able to block the cell mitotic progression and ultimately induced apoptosis preventing proliferation of damaged cells. Indeed, RAPTA-T affects cell cycle progression in a similar way to other ruthenium complexes [23, 27, 35, 42]. The upregulation of cyclin B and a significant decrease of total Cdc2, due to the lack of Cdc25 phosphatase activity, suggests that these changes in the proteins involving in cell cycle regulation in G2/M phase may be linked to RAPTA-T treatment [47, 48]. In addition, RAPTA-C inhibits cell cycle progression at the G2/M phase by increasing p21 expression in a p53-dependent manner and the subsequent apoptosis [23]. The pronounced differences in sensitivity to RAPTA-T in both types of breast cancer cells were observed. A higher extent of G2/M in the HCC1937 cells that harbors a BRCA1 mutation (5382insC) might be related to dysfunctional BRCA1 that is unable to repair DNA damage produced by RAPTA-T, resulting in accumulation of genomic instability, and ultimately to apoptotic cell death

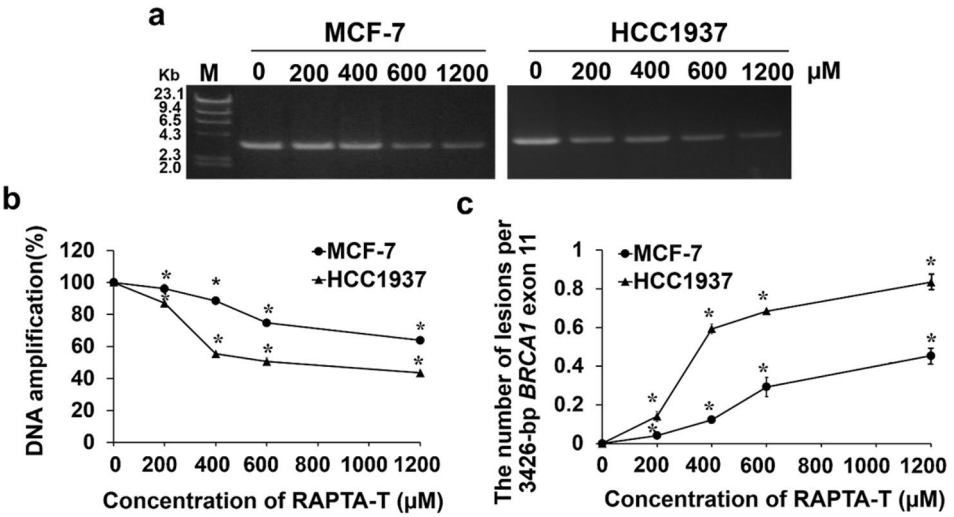

Fig. 6 Cellular *BRCA1* damage in MCF-7 and HCC1937 cells (**a**). Cells were incubated with various concentrations of RAPTA-T (200–1200 μM) for 48 h. Genomic DNA of ruthenium-treated or untreated (control) cells was isolated and the 3426 bp *BRCA1* exon 11 fragment was then amplified by the PCR reaction, and the PCR products were electrophoresed on 1% agarose gel. The gel was stained with ethidium bromide and visualized under UV illumination. M stands for λ-HindIII digested marker. Amplification products were quantified band intensity using a Bio-Rad Molecular Imager. The amount of DNA amplification (%) was plotted as a function of concentration (**b**). The lesion frequently per the 3426 bp fragment of the *BRCA1* exon 11 by RAPTA-T calculated by the Poisson equation (**c**) [36]. The standard error of experiments realized in duplicate was plotted. Statistical significance differences from the untreated control are indicated by $*p < 0.01$

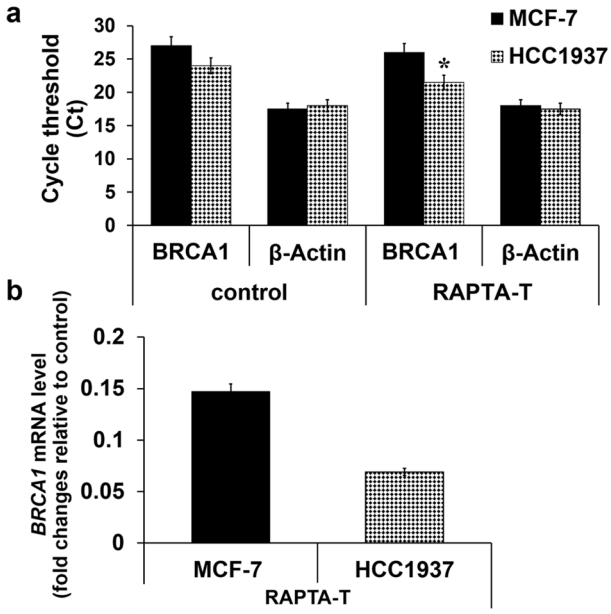

Fig. 7 Effect of RAPTA-T on *BRCA1* mRNA expression in MCF-7 and HCC1937 cells. Cells were incubated in the absence and the presence of 1 mM of RAPTA-T for 48 h. The expression level of *BRCA1* mRNA was determined by a real-time quantitative RT-PCR. The data were analyzed according to the 2-ΔΔCq method [37] and normalized to the β-actin reference gene expression and relative to the respective expression of untreated control. **a** Cycle threshold (Ct) and **b** fold change for *BRCA1* mRNA expression in MCF-7 and HCC1937 cells relative to the control. The data are expressed as the mean ± SD of three individual experiments

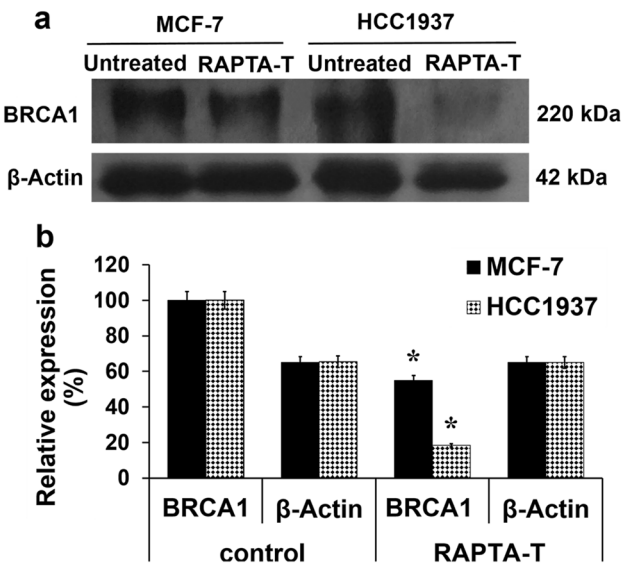

Fig. 8 Effect of RAPTA-T on BRCA1 protein expression in MCF-7 and HCC1937 cells (**a**). Whole-cell proteins were prepared from the cells treated with 1 mM of RAPTA-T for 48 h. Cellular protein extracts were separated on a 6% SDS-PAGE gel, transferred onto nitrocellulose membrane, and immunoblotted with the anti-BRCA1 antibody. The protein loading of each sample was controlled by β-actin expression using anti β-actin. Relative expression of BRCA1 protein (%) in MCF-7 and HCC1937 cells (**b**). Experiments were performed in triplicate. Statistically significant differences from the untreated control are indicated by $*p < 0.01$

[49]. The cytotoxicity of some ruthenium complexes has been correlated with their ability to induce DNA damage that leads to the inhibition of DNA replication, transcription, and ultimately to programmed cell death with similar kinetics to cisplatin [50]. Recently, damage to the *BRCA1* gene in cancer cells has received much attention as a potential molecular target for metal-based anticancer compounds [33, 35, 36, 39, 40, 51]. RAPTA-T is able to inhibit *BRCA1* replication in a dose-dependent manner. However, at equal doses, RAPTA-T causes much more *BRCA1* damage in HCC1937 cells compared to MCF-7 cells. Notably, the level of lesions within specified *BRCA1* fragment in MCF-7 cells were lower than in HCC1937 cells, whereas the accumulation of ruthenium in nuclear fraction in MCF-7 cells was significantly higher than in HCC1937 cells. Consequently, it is possible that RAPTA-T forms adducts with specific histone sites on the nucleosome core rather than binding to genomic DNA [42]. Interestingly, *BRCA1* mRNA and its protein in *BRCA1*-defective HCC1937 cells are dramatically decreased following treatment with RAPTA-T. This could be attributed to the ruthenation of the *BRCA1* gene that can interfere with DNA replication, transcription and translation [33], and might lead to an insufficient of BRCA1 function in cancer cells. In clinical studies, it has been shown that the response of cancer patients to cisplatin depends on the status or expression of *BRCA1* mRNA and its protein. Patient with low or intermediate levels of BRCA1 expression were found to be hypersensitive to cisplatin, whereas enhanced resistance to cisplatin was observed in those with over-expression of the BRCA1 protein [51, 52].

In conclusion, we have investigated the cellular responses of *BRCA1*-defective HCC1937 breast cancer cells induced by the antimetastasis compound RAPTA-T. RAPTA-T was essentially nontoxic to *BRCA1*-defective HCC1937 and *BRCA1*-competent MCF-7 cells, with the ruthenium localized mainly in the cytoplasm of both cell lines. However, RAPTA-T showed different cellular responses to both cell lines depending on the BRCA1 status. RAPTA-T mediated inhibition of cell growth through triggering cell cycle arrest at G2/M that lead to apoptosis. Moreover, it causes dramatic cellular *BRCA1* damage in *BRCA1*-defective HCC1937 cells with the subsequent down-regulation of *BRCA1* mRNA and its protein. Consequently, RAPTA-T could be a useful drug for the treatment of *BRCA1*-defective breast cancers when applied in combination with other agents that exhibit complementary modes of action.

Acknowledgements This research work was supported by the National Research Council of Thailand (PHA610093S and PHA590396S), Prince of Songkla University (PHA6202079S), and the Graduate school, Prince of Songkla University. We would like to thank the Pharmaceutical Laboratory Service Center and Department of Pharmaceutical Chemistry, Faculty of Pharmaceutical Sciences, Prince of Songkla University for providing research facilities.

Compliance with ethical standards

Conflict of interest The authors declare that they have no conflicts of interest.

Human and animal rights The article does not contain any studies with human participants or animals performed by any of the authors.

References

1. Siegel RL, Miller KD, Jemal A (2016) Cancer statistics: 2016. CA Cancer J Clin 66:7–30. https://doi.org/10.3322/caac.21332
2. Li Y, Li S, Chen J et al (2014) Comparative epigenetic analyses reveal distinct patterns of oncogenic pathways activation in breast cancer subtypes. Hum Mol Genet 23:5378–5393. https://doi.org/10.1093/hmg/ddu256
3. Perou CM, Sørlie T, Eisen MB et al (2000) Molecular portraits of human breast tumours. Nature 406:747–752. https://doi.org/10.1038/35021093
4. Severson TM, Peeters J, Majewski I et al (2015) BRCA1-like signature in triple negative breast cancer: molecular and clinical characterization reveals subgroups with therapeutic potential. Mol Oncol 9:1528–1538. https://doi.org/10.1016/j.molonc.2015.04.011
5. Bhattacharyya A, Ear US, Koller BH, Weichselbaum RR, Bishop DK (2000) The breast cancer susceptibility gene BRCA1 is required for subnuclear assembly of Rad51 and survival following treatment with the DNA cross-linking agent cisplatin. J Biol Chem 275:23899–23903. https://doi.org/10.1074/jbc.C000276200
6. Elstrodt F, Hollestelle A, Nagel JH et al (2006) BRCA1 mutation analysis of 41 human breast cancer cell lines reveals three new deleterious mutants. Cancer Res 66:41–45. https://doi.org/10.1158/0008-5472.CAN-05-2853
7. Tassone P, Tagliaferri P, Perricelli A et al (2003) BRCA1 expression modulates chemosensitivity of BRCA1-defective HCC1937 human breast cancer cells. Br J Cancer 88:1285–1291. https://doi.org/10.1038/sj.bjc.6600859
8. Domagala P, Huzarski T, Lubinski J, Gugala K, Domagala W (2011) Immunophenotypic predictive profiling of BRCA1-associated breast cancer. Virchows Arch 458:55–64. https://doi.org/10.1007/s00428-010-0988-3
9. Esteller M, Silva JM, Dominguez G et al (2000) Promoter hypermethylation and BRCA1 inactivation in sporadic breast and ovarian tumors. J Natl Cancer Inst 92:564–569. https://doi.org/10.1093/jnci/92.7.564
10. Stefansson OA, Villanueva A, Vidal A, Martí L, Esteller M (2012) BRCA1 epigenetic inactivation predicts sensitivity to platinum-based chemotherapy in breast and ovarian cancer. Epigenetics 7:1225–1229. https://doi.org/10.4161/epi.22561
11. Veeck J, Ropero S, Setien F et al (2010) BRCA1 CpG island hypermethylation predicts sensitivity to poly(adenosine diphosphate)-ribose polymerase inhibitors. J Clin Oncol 28:563–564. https://doi.org/10.1200/JCO.2010.30.1010
12. Font A, Taron M, Gago JL et al (2011) BRCA1 mRNA expression and outcome to neoadjuvant cisplatin-based chemotherapy in bladder cancer. Ann Oncol 22:139–144. https://doi.org/10.1093/annonc/mdq333
13. Isakoff SJ, Mayer EL, He L et al (2015) TBCRC009: a multicenter phase II clinical trial of platinum monotherapy with biomarker assessment in metastatic triple-negative breast cancer. J Clin Oncol 33:1902–1909. https://doi.org/10.1200/JCO.2014.57.6660
14. Carozzi VA, Marmiroli P, Cavaletti G (2010) The role of oxidative stress and anti-oxidant treatment in platinum-induced peripheral

neurotoxicity. Curr Cancer Drug Targets 10:670–682. https://doi.org/10.2174/156800910793605820
15. Tezcan S, Izzettin FV, Sancar M, Yumuk PF, Turhal S (2013) Nephrotoxicity evaluation in outpatients treated with cisplatin-based chemotherapy using a short hydration method. Pharmacol Pharm 4:296–302. https://doi.org/10.4236/pp.2013.43043
16. Dhillon KK, Swisher EM, Taniguchi T (2011) Secondary mutations of BRCA1/2 and drug resistance. Cancer Sci 102:663–669. https://doi.org/10.1111/j.1349-7006.2010.0
17. Swisher EM, Sakai W, Karlan BY, Wurz K, Urban N, Taniguchi T (2008) Secondary BRCA1 mutations in BRCA1-mutated ovarian carcinomas with platinum resistance. Cancer Res 68:2581–2586. https://doi.org/10.1158/0008-5472.CAN-08-0088
18. Hongthong K, Ratanaphan A (2016) *BRCA1*-associated triple-negative breast cancer and potential treatment for ruthenium-based compounds. Curr Cancer Drug Targets 16:606–617. https://doi.org/10.2174/1568009616666160203113957
19. Bergamo A, Gaiddon C, Schellens JH, Beijnen JH, Sava G (2012) Approaching tumour therapy beyond platinum drugs: status of the art and perspectives of ruthenium drug candidates. J Inorg Biochem 106:90–99. https://doi.org/10.1016/j.jinorgbio.2011.09.030
20. Leijen S, Burgers SA, Baas P et al (2015) Phase I/II study with ruthenium compound NAMI-A and gemcitabine in patients with non-small cell lung cancer after first line therapy. Invest New Drugs 33:201–214. https://doi.org/10.1007/s10637-014-0179-1
21. Murray BS, Babakb MV, Hartingerb CG, Dyson PJ (2016) The development of RAPTA compounds for the treatment of tumors. Coord Chem Rev 306:86–114. https://doi.org/10.1016/j.ccr.2015.06.014
22. Scolaro C, Bergamo A, Brescacin L et al (2005) In vitro and in vivo evaluation of ruthenium(II)-arene PTA complexes. J Med Chem 48:4161–4171. https://doi.org/10.1021/jm050015d
23. Chatterjee S, Kundu S, Bhattacharyya A, Hartinger CG, Dyson PJ (2008) The ruthenium(II)-arene compound RAPTA-C induces apoptosis in EAC cells through mitochondrial and p53-JNK pathways. J Biol Inorg Chem 13:1149–1155. https://doi.org/10.1007/s00775-008-0400-9
24. Weiss A, Berndsen RH, Dubois M et al (2014) In vivo anti-tumor activity of the organometallic ruthenium(II)-arene complex [Ru(η6-p-cymene)Cl2(pta)] (RAPTA-C) in human ovarian and colorectal carcinomas. Chem Sci 5:4742–4748. https://doi.org/10.1039/C4SC01255K
25. Weiss A, Bonvin D, Berndsen RH et al (2015) Angiostatic treatment prior to chemo-or photodynamic therapy improves anti-tumor efficacy. Sci Rep 5:8990. https://doi.org/10.1038/srep08990
26. Weiss A, Ding X, van Beijnum JR et al (2015) Rapid optimization of drug combinations for the optimal angiostatic treatment of cancer. Angiogenesis 18:233–244. https://doi.org/10.1007/s10456-015-9462-9
27. Adhireksan Z, Davey GE, Campomanes P et al (2014) Ligand substitutions between ruthenium-cymene compounds can control protein versus DNA targeting and anticancer activity. Nat Commun 5:3462–3475. https://doi.org/10.1038/ncomms4462
28. Wu B, Ong MS, Groessl M et al (2011) A ruthenium antimetastasis agent forms specific histone protein adducts in the nucleosome core. Chemistry 17:3562–3566. https://doi.org/10.1002/chem.201100298
29. Groessl M, Tsybin YO, Hartinger CG, Keppler BK, Dyson PJ (2010) Ruthenium versus platinum: interactions of anticancer metallodrugs with duplex oligonucleotides characterised by electrospray ionisation mass spectrometry. J Biol Inorg Chem 15:677–688. https://doi.org/10.1007/s00775-010-0635-0
30. Nowak-Sliwinska P, van Beijnum JR, Casini A et al (2011) Organometallic ruthenium(II) arene compounds with antiangiogenic activity. J Med Chem 54:3895–3902. https://doi.org/10.1021/jm2002074
31. Bergamo A, Masi A, Dyson PJ, Sava G (2008) Modulation of the metastatic progression of breast cancer with an organometallic ruthenium compound. Int J Oncol 33:1281–1289. https://doi.org/10.3892/ijo_00000119
32. Lee RFS, Chernobrovkin A, Rutishauser D et al (2017) Expression proteomics study to determine metallodrug targets and optimal drug combinations. Sci Rep 7:1590. https://doi.org/10.1038/s41598-017-01643-1
33. Ratanaphan A, Nhukeaw T, Hongthong K, Dyson PJ (2017) Differential cytotoxicity, cellular uptake, apoptosis and inhibition of BRCA1 expression of BRCA1-defective and sporadic breast cancer cells induced by an anticancer ruthenium(II)-arene compound, RAPTA-EA1. Anticancer Agents Med Chem 17:212–220. https://doi.org/10.2174/1871520616666160404110953
34. Koch RB (1969) Fractionation of olfactory tissue homogenates. Isolation of a concentrated plasma membrane fraction. J Neurochem 16:145–157. https://doi.org/10.1111/j.1471-4159.1969.tb05933.x
35. Nhukeaw T, Temboot P, Hansongnern K, Ratanaphan A (2014) Cellular responses of BRCA1-defective and triple-negative breast cancer cells and in vitro BRCA1 interactions induced by metallo-intercalator ruthenium(II) complexes containing chloro-substituted phenylazopyridine. BMC Cancer 14:73. https://doi.org/10.1186/1471-2407-14-73
36. Ratanaphan A, Canyuk B, Wasiksiri S, Mahasawat P (2005) In vitro platination of human breast cancer suppressor gene1 (BRCA1) by the anticancer drug carboplatin. Biochim Biophys Acta 1725:145–151. https://doi.org/10.1016/j.bbagen.2005.07.006
37. Livak KJ, Schmittgen TD (2001) Analysis of relative gene expression data using real-time quantitative PCR and the 2(-Delta Delta C(T)) Method. Method 25:402–408. https://doi.org/10.1006/meth.2001.1262
38. Babak MV, Meier SM, Huber KVM et al (2015) Target profiling of an antimetastatic RAPTA agent by chemical proteomics: relevance to the mode of action. Chem Sci 6:2449–2456. https://doi.org/10.1039/c4sc03905j
39. Chakree K, Ovatlarnporn C, Dyson PJ, Ratanaphan A (2012) Altered DNA binding and amplification of human breast cancer suppressor gene BRCA1 induced by a novel antitumor compound, [Ru(η^6-*p*-phenylethacrynate)Cl_2(pta)]. Int J Mol Sci 13:13183–13202. https://doi.org/10.3390/ijms131013183
40. Ratanaphan A, Temboot P, Dyson PJ (2010) In vitro ruthenation of human breast cancer suppress or gene 1 (BRCA1) by the antimetastasis compound RAPTA-C and its analogue CarboRAPTA-C. Chem Biodivers 7:1290–1302. https://doi.org/10.1002/cbdv.200900288
41. Groessl M, Terenghi M, Casini A, Elviri L, Lobinski R, Dyson PJ (2010) Reactivity of anticancer metallodrugs with serum proteins: new insights from size exclusion chromatography-ICP-MS and ESI-MS. J Anal At Spectrom 25:305–313. https://doi.org/10.1039/B922701F
42. Wolters DA, Stefanopoulou M, Dyson PJ, Groessl M (2012) Combination of metallomics and proteomics to study the effects of the metallodrug RAPTA-T on human cancer cells. Metallomics 4:1185–1196. https://doi.org/10.1039/c2mt20070h
43. Gavande NS, VanderVere-Carozza PS, Hinshaw HD et al (2016) DNA repair targeted therapy: the past or future of cancer treatment? Pharmacol Ther 160:65–83. https://doi.org/10.1016/j.pharmthera.2016.02.003
44. Mendes F, Groessl M, Nazarov AA et al (2011) Metal-based inhibition of poly(ADP-ribose) polymerase-the guardian angel of DNA. J Med Chem 54:2196–2206. https://doi.org/10.1021/jm2000135
45. Temboot P, Lee RFS, Menin L, Patiny L, Dyson PJ, Ratanaphan A (2017) Biochemical and biophysical characterization of ruthenation of BRCA1 RING protein by RAPTA complexes and

its E3 ubiquitin ligase activity. Biochem Biophys Res Commun 488:355–361. https://doi.org/10.1016/j.bbrc.2017.05.052
46. Adhireksan Z, Palermo G, Riedel T et al (2017) Allosteric crosstalk in chromatin can mediate drug-drug synergy. Nat Commun 8:14806–14817. https://doi.org/10.1038/ncomms14860
47. Bergamo A, Gagliardi R, Scarcia V et al (1999) In vitro cell cycle arrest, in vivo action on solid metastasizing tumors, and host toxicity of the antimetastatic drug NAMI-A and cisplatin. J Pharmacol Exp Ther 289:559–564
48. Zajac M, Moneo MV, Carnero A, Benitez J, Martínez-Delgado B (2008) Mitotic catastrophe cell death induced by heat shock protein 90 inhibitor in BRCA1-deficient breast cancer cell lines. Mol Cancer Ther 7:2358–2366. https://doi.org/10.1158/1535-7163.MCT-08-0327
49. Tassone P, Di Martino MT, Ventura M et al (2009) Loss of BRCA1 function increases the antitumor activity of cisplatin against human breast cancer xenografts in vivo. Cancer Biol Ther 8:648–653. https://doi.org/10.4161/cbt.8.7.7968
50. Brabec V, Nováková O (2006) DNA binding mode of ruthenium complexes and relationship to tumor cell toxicity. Drug Resist Updat 9:111–122. https://doi.org/10.1016/j.drup.2006.05.002
51. James CR, Quinn JE, Mullan PB, Johnston PG, Harkin DP (2007) BRCA1, a potential predictive biomarker in the treatment of breast cancer. Oncologist 12:142–150. https://doi.org/10.1634/theoncologist.12-2-142
52. Lohse I, Borgida A, Cao P et al (2015) BRCA1 and BRCA2 mutations sensitize to chemotherapy in patient-derived pancreatic cancer xenografts. Br J Cancer 113:425–432. https://doi.org/10.1038/bjc.2015.220